International Journal of Refractory Metals and Hard Materials 98 (2021) 105529

Contents lists available at ScienceDirect

International Journal of Refractory Metals and Hard Materials

journal homepage: www.elsevier.com/locate/IJRMHM

Measuring the fracture toughness of single WC grains of cemented carbides by means of microcantilever bending and micropillar splitting

L. Ortiz-Membrado [a], N. Cuadrado [b], D. Casellas [b,c], J.J. Roa [a,d], L. Llanes [a,d], E. Jiménez-Piqué [a,d,*]

[a] CIEFMA - Department of Materials Science and Engineering, EEBE, Universitat Politècnica de Catalunya-BarcelonaTECH, Avda. Eduard Maristany 16, 08019 Barcelona, Spain
[b] Eurecat, Centre Tecnològic de Catalunya, Unit of Metallic and Ceramic Materials, Plaça de la Ciència, 2, Manresa 08243, Spain
[c] Division of Mechanics of Solid Materials, Lulea University of Technology, 971 87 Lulea, Sweden
[d] Barcelona Research Center in Multiscale Science and Engineering- Universitat Politècnica de Catalunya-BarcelonaTECH, Avda. Eduard Maristany 16, 08019 Barcelona, Spain

ARTICLE INFO

Keywords:
Fracture toughness
WC grains
Mechanical properties
Micromechanical testing

ABSTRACT

The main goal of this work is to obtain a reliable value of the fracture toughness of single grains of tungsten carbide (WC). It is attempted by testing microcantilever and micropillar samples shaped out, by means of focused ion beam milling, of individual WC particles embedded within a WC-Co cemented carbide grade. Experimental testing included the use of a nanoindenter for inducing microcantilever bending and micropillar splitting, as well as sampling WC grains with basal and prismatic orientations. Experimental results are compared with those previously assessed through implementation of the indentation microfracture technique. Bending of notched microcantilevers yielded more consistent results than those measured out of micropillar splitting tests. In this regard, the average value of fracture toughness for single WC grains, within the two-phase interpenetrated network existing in cemented carbides, is found to be 5.6 ± 0.8 MPa·m$^{1/2}$. Such a relatively high value – coherent with local plastic features evidenced in nanoindentation imprints - is in satisfactory agreement with results indirectly estimated from other macromechanical tests.

1. Introduction

Cemented carbides, also referred as a hardmetals, are materials widely used as cutting, forming and machining tools in a broad range of industrial applications [1]. Main reason behind it is the exceptional combination of strength, toughness and wear resistance that they exhibit, as a direct consequence of the extremely different chemical nature of their constitutive phases: hard ceramic particles (usually WC) and a soft metallic binder (commonly a Co- or Ni-based alloy). Mechanical properties of these ceramic-metal composites, especially hardness and fracture toughness, depend on phase content, effective size of each microstructural constituent, type of binder and intrinsic properties of the carbides [2,3].

Failure of cemented carbides components frequently involve wear or contact-related phenomena, fracture and/or fatigue of the material [4–12]. All these mechanisms involve cracking of single WC grains which can either trigger the propagation of existing flaws or induce loss of material integrity in the case of wear. Hence, in-depth knowledge about the fracture toughness of individual carbides will result in a better understanding on how failure takes place in cemented carbides; and thus, on how the performance of tools and components made of these materials may be enhanced. Moreover, the intrinsic mechanical properties of single phases are of special relevance as robust inputs for numerical simulation of composites.

A method usually invoked to measure fracture toughness at small length scales for brittle-like materials is the one referred to as Indentation Microfracture method (IM). It is based on the formation of cracks at the corners of an imprint induced after applying load using a sharp indenter, i.e. Vickers, Berkovich or cube-corner diamond tips. These indentation cracks extend, driven by the inelastic residual stress field, up to a length that can be related to the resistance to crack propagation of the material. Sharper indenters as the cube-corner ones, displace a much

* Corresponding authorat: CIEFMA - Department of Materials Science and Engineering, EEBE, Universitat Politècnica de Catalunya-BarcelonaTECH, Avda. Eduard Maristany 16, 08019 Barcelona, Spain.
E-mail address: emilio.jimenez@upc.edu (E. Jiménez-Piqué).

https://doi.org/10.1016/j.ijrmhm.2021.105529
Received 9 March 2021; Received in revised form 17 March 2021; Accepted 18 March 2021
Available online 24 March 2021

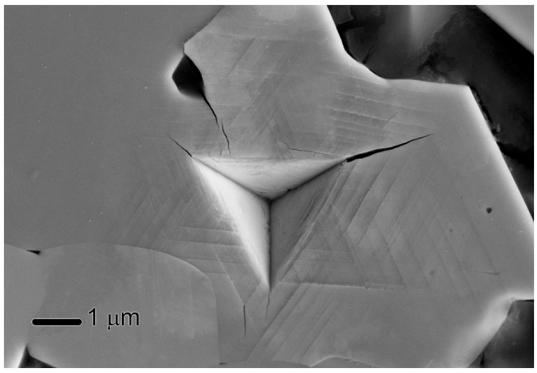

Fig. 1. Typical cube-corner indentation of a single WC grain. Observe that the large amount of plasticity induced by the indentation as well as the presence of secondary cracks.

larger volume of material for a given load; therefore, higher stresses are induced beneath the indenter. As a consequence, cracks can be generated at lower loads [13,14]. In general, the IM method is quite popular and extensively used, mainly because it is not only easy and inexpensive, but also especially useful for acquiring toughness-like data in small volumes of material, as far as all the assumptions prescribed by its use and analysis are fullfiled (e.g. Refs. [15–18]). However, criticisms to the IM method point that this technique is not suitable for the precise measurement of fracture toughness [19], as it just measures an indentation fracture resistance which is latter fitted through calibration constants to the value of K_{Ic}. Moreover, for the particular case of WC grains, it has been reported that crack shape produced by cube corner indenters deviates from the assumed shape [20], and this can introduce deviations of the measured K_{Ic} value. Therefore, although an estimation of K_{Ic} can be done by IM methods, accurate K_{Ic} measurements require a proper knowledge of the crack morphology which depends on the indentation load, tip geometry, material toughness and crystal anisotropy.

In a previous work of the authors, the IM method with cube corner indenters was implemented for assessment of fracture toughness values (K_{Ic}) of single WC grains. Attained values of K_{Ic} were 8.7 ± 1.1 MPa·m$^{1/2}$ and 7.2 ± 2.4 MPa·m$^{1/2}$ when indentations were done on prismatic and basal faces respectively [21]. These measurements were experimentally difficult to analyse because plastic deformation induced by the indentations performed was quite noticeable (see Fig. 1). As a consequence, cracks emanating from imprint corners deviated from the ideal shape, as assumed in the models. It is then believed that these anisotropic effects in the crack patterns as well as the irreversible deformation mechanisms activated could have led to an inaccurate estimation of K_{Ic} of the studied WC grains.

Following the above ideas, the objective of this work is to evaluate K_{Ic} of single WC grains, within the characteristic phase assemblage evidenced in cemented carbides, by the implementation of techniques using notched microcantilevers and micropillars, milled by focused ion beam (FIB). Although these techniques are clearly more time consuming, they are more robust for reliable measurement of the fracture toughness of a brittle-like material at small length scales.

Microcantilever bending and micropillar splitting methods have been used for investigating fracture behaviour of brittle materials and coatings at small scales. Regarding the former, with the flexibility of FIB instruments enabling a variety of possible testing setups, many different cantilever geometries have been reported in literature [22–27]. During cantilever bending (induced through loading applied by means of a diamond tip within a nanoindenter unit), cleavage and instantaneous cracking may occur for many brittle materials, enabling then the measurement of K_{Ic}. Similar to microcantilever bending, sharp nanoindentation is also key for measurement of K_{Ic} using the micropillar splitting method. It is done on the top surface of a FIB-milled micropillar. After initial loading, a crack nucleates underneath the sharp indenter which produces a pop-in in the load displacement curve. Once a critical load is reached, the crack extends out to the pillar surface [28–30]. The advantage of this method is that it does not require to produce an initial notch.

Both techniques have the advantage that potential residual stresses are released by the FIB milling process; and thus, they are not expected to affect the result. This is important in WC grains embedded in a hardmetal phase assemblage, where it is known that hard particles exhibit microresidual compressive stresses in the order of 500 MPa [31,32].

In this study, K_{Ic} values attained using both methods are compared against each other, as well as with those obtained using the IM technique (using a cube-corner indentation tip). Results are then discussed, aiming to document and highlight the relative advantages and drawbacks, in terms of reliability of the K_{Ic} values measured.

2. Methods used to evaluate fracture toughness at small length scale: Testing and data analysis

2.1. Microcantilever bending

Testing of this geometry is similar to the procedure followed during macroscale cantilever bending. Considering the small length scale involved, a cantilever must be first milled by FIB. Such process includes the introduction of a notch with known depth near the clamped edge. Once this is done, the notched microcantilever is then bended using a nanoindenter, with enough spatial and load resolution, in the other side. Because the limitations of the FIB-milled geometries, cantilevers are usually shaped with an irregular pentagon geometry, also known as house shape. A scheme of this geometry is presented in Fig. 1.

The fracture toughness may then be calculated using the following equation:

$$K_{Ic} = \sigma \sqrt{\pi a}\, F\left(\frac{a}{b}\right) \tag{1}$$

where σ is the fracture stress, a is the notch depth and $F(a/b)$ the shape factor. The corresponding fracture stress is assessed by introducing the experimentally determined fracture load P in the equation:

$$\sigma = \frac{PLy}{I} \tag{2}$$

where L the distance between the notch location and the point where the force is applied, y is the vertical distance between the upper surface and the neutral plane, as defined by:

$$y = \frac{\frac{wb^2}{2} + \frac{w^2}{4}\left(b + \frac{w}{3}\right)}{bw + \frac{w^2}{4}} \tag{3}$$

and I is the moment of inertia of the beam cross section, which is given by:

$$I = \frac{wb^3}{12} + \left(y - \frac{b}{2}\right)^2 bw + \frac{w^4}{288} + \left(\frac{b}{6} + (b - y)\right)^2 \frac{w^4}{4} \tag{4}$$

here b and w are the thickness and the width, respectively, of the rectangular portion of the cantilever.

The dimensionless shape factor, $F(a/b)$, may be calculated by using the equation provided by Di Maio and Roberts [22], valid for $0.3 \leq \left(\frac{a}{b}\right) \leq 0.5$, as follows:

$$F\left(\frac{a}{b}\right) = 1.85 - 3.38\left(\frac{a}{b}\right) + 13.24\left(\frac{a}{b}\right)^2 - 23.26\left(\frac{a}{b}\right)^3 + 16.8\left(\frac{a}{b}\right)^4 \tag{5}$$

Table 1
Hardness and Young's modulus of WC grains as a function of their crystallographic orientation [21].

Crystallographic orientation	H [GPa]	E [GPa]
Prismatic facet	17.2 ± 0.1	564 ± 26
Basal facet	25.6 ± 0.2	532 ± 23

2.2. Micropillar splitting

The micropillar splitting method for determining K_{Ic} of ceramic films was developed by Sebastiani et al. [29]. Here, a pillar with an aspect ratio (height/diameter) larger than one is milled, and then indented in the middle of its top surface with a sharp nanoindentation tip. Fracture is detected by a pop-in in the load-displacement curve. The load of this first pop-in, P_c, is then used to calculate the K_{Ic} of the material, by using the following equation:

$$K_{Ic} = \gamma \frac{P_c}{R^{3/2}} \tag{6}$$

where R is the radius of the pillar and γ is a calibration coefficient which depends on the hardness/Young's modulus of the material [33].

2.3. Indentation microfracture method

For small volumes, this method is based on the use of a cube-corner indenter to produce an imprint at a given load (P). The length of the cracks emanating from the corners of the induced imprint are then measured. Assuming that a Palmqvist crack system is developed, typical of cemented carbides [34], K_{Ic} can be calculated as:

$$K_{Ic} = \chi_v \left(\frac{E}{H}\right)^{2/3} \left(\frac{a}{l}\right)^{1/2} \frac{P}{c^{3/2}} \tag{7}$$

where P is the indentation load, c is the crack length, a is the half-diagonal of the indentation impression, E is the Young's modulus, H is the hardness and χ_v is a constant empirically determined that depends on the crack geometry (0.015 for WC [16]).

3. Experimental procedure

A commercial WC-Co cemented carbide grade was used. Mean grain size of WC and binder content were about 20 μm and 8.5 wt% respectively. Hardness and Young's modulus for each crystal orientation of WC grains [21] studied are listed in Table 1. An extra-coarse hardmetal grade was chosen in order to mill the necessary features with large enough dimensions.

WC grains were selected in basal and prismatic orientations by Electron Backscatter Diffraction (EBSD). Samples were mechanically polished to mirror surface finish with a 0.05 μm colloidal silica suspension. The EBSD measurements were performed at 20 kV with a step size of 0.2 μm. The analysed areas were 500 × 500 μm^2. All data was collected using a Nordlys camera from Oxford Instruments on a Zeiss Field Emission Scanning Electron Microscopy (FE-SEM). Specimens were milled using a FIB (Carl Zeiss Neon40 Crossbeam) operated at 30 kV. Several steps with different intensities were done in order to obtain the final geometry. The last current used to refine was 500 pA and 2 nA for micropillars and microcantilevers, respectively. Pillars of 3 and 5 μm of diameter with an aspect ratio ≥ 1 were milled. Cantilevers with a width of 20 μm, a height of 25 μm and a depth of 15 μm approximately, were milled to create the house-shape cross section with a 45° angle (see Fig. 1). For introducing the notch, a line was carved using the mill in time mode with a current of 100 pA during 35 s. Testing of materials was done using a MTS Nanoindenter XP.

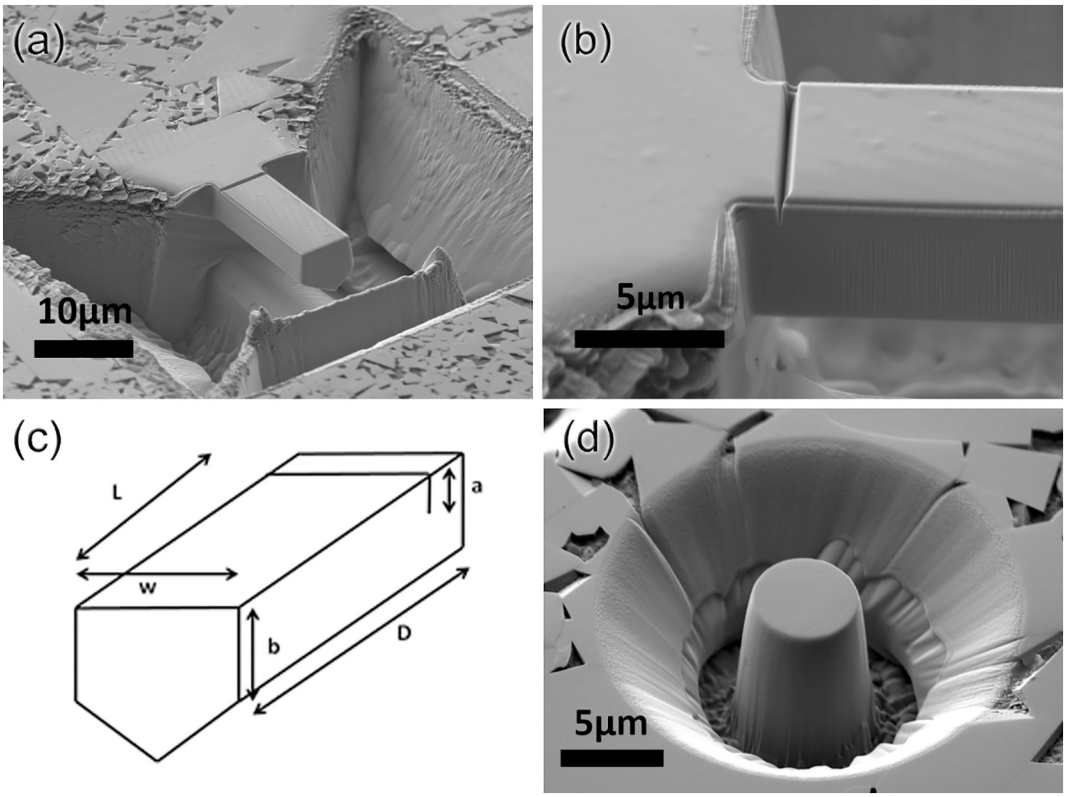

Fig. 2. Produced geometries for testing. (a(Typical micro-cantilever in a WC single grain, (b) of the machined notch, (c) scheme of the labels used for the dimensions of the micro-cantilevers and (d) pillar machined in a single WC grain.

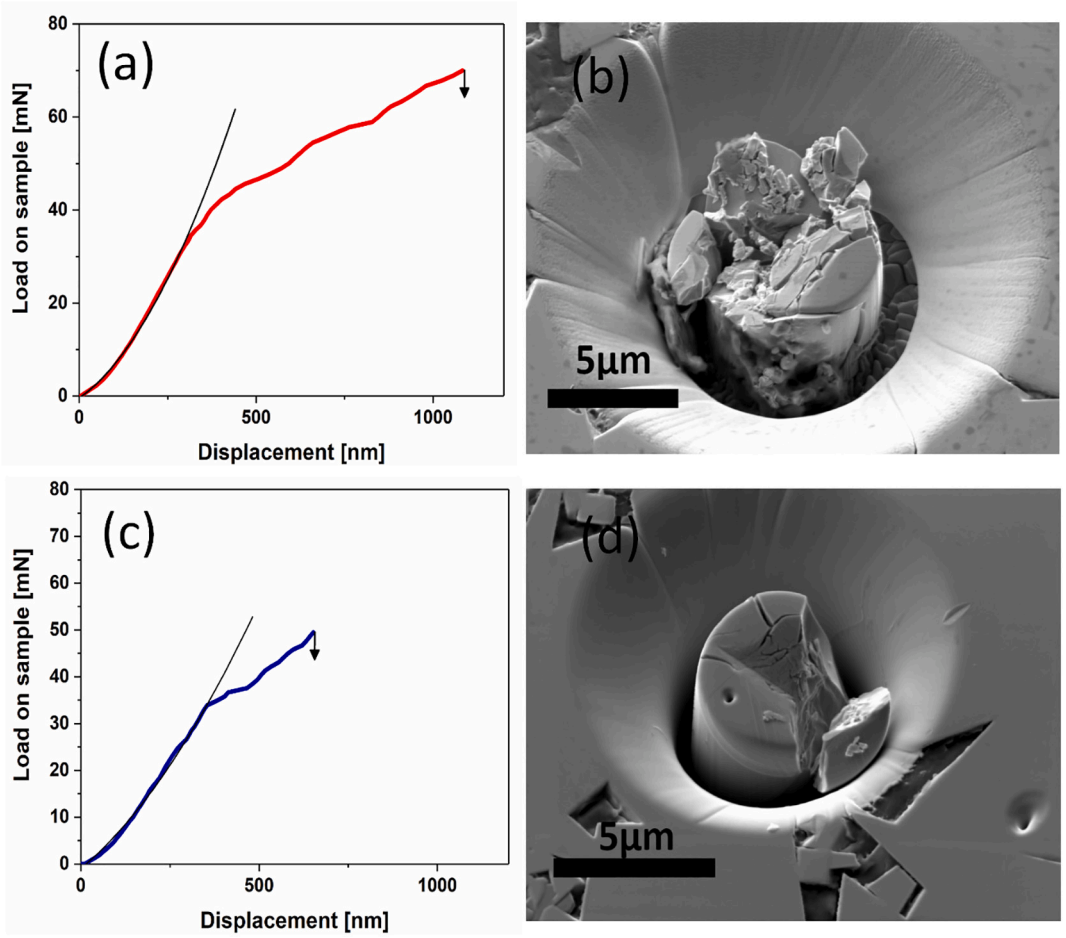

Fig. 3. load-displacement curves and SEM images of pillars after splitting, of prismatic (a) and (b) and basal (c) and (d) orientations.

4. Results and discussion

Fig. 2 shows images of samples milled, before being tested. Representative load-displacement curves together with typical micrographs of fractured samples are shown in Figs. 3 and 4

All the samples milled and tested, including crystallographic orientation (prismatic or basal) and dimensions, as well as the experimentally determined critical loads and calculated K_{Ic} values for each test are listed in Tables 2 and 3.

In addition, all the K_{Ic} results, including those obtained by IM in a previous work [21], are presented – as a function of crystallographic orientation – in a single plot for comparison purposes in Fig. 5 Average values are also presented in Table 4.

From Fig. 5 it is seen that the three testing methods considered yield different results. Micropillar splitting tests give the lowest values, ranging between 1.5 and 6.0 MPa·m$^{1/2}$. Higher values - between 5.0 and 6.4 MPa·m$^{1/2}$ - are attained from microcantilever bending tests. However, they are still lower than the ones previously reported using the IM method, i.e. between 7.2 and 8.7 MPa·m$^{1/2}$. Moreover, direct comparison of the results attained from implementation of micropillar and microcantilever methods shows that the former exhibits a larger scatter and a more noticeable difference between prismatic and basal orientations than the latter. Indeed, with the current set of experiments, crystal orientation effects on K_{Ic} are not discerned by using the microcantilever bending method. Nevertheless, additional research efforts in this subject (e.g. by testing a larger number of specimens) are suggested to confirm the observed experimental relationship.

Calculation of K_{Ic} values from experimental data recorded during micropillar splitting tests requires pillars to become fractured in a symmetric way. Accordingly, validation of the estimated results may be assessed by checking the number of fragments in which pillars got broken. Considering that indentation imprints were induced by a cube-corner diamond tip, micropillars should have fractured in three pieces. However, close inspection of the broken pillars indicate that this was seldom the case. In general, micropillars were found to split following just one of the induced indentation cracks. Furthermore, in several cases induced cracks did not follow radial directions from the vertices of the imprint. Such a finding may be rationalized considering that WC exhibits pronounced anisotropy in its plastic behaviour, due to its hexagonal crystal structure (e.g. Refs. [35, 36]). It implies a more favourable crack propagation along specific directions. Hence, such significant plastic anisotropy is indirectly responsible for the extreme crystal orientations effects observed when analysing the results attained by means of the micropillar splitting method.

Different from the methods where indentation imprints; and thus, localized plastic deformation features, are involved, fracture phenomena evidenced in microcantilever bending tests may be described as purely brittle. Loading-displacement curves were linear until sudden failure, and resulting fracture surfaces appeared to be smooth. In these tests, validation of the attained results requires linear elastic fracture conditions to be satisfied, i.e. plastic zone at the crack tip to be much smaller than crack length. Size of the crack tip (r_p) is related to yield stress (σ_y) and fracture toughness, as follows:

$$r_P = \frac{{K_{IC}}^2}{2\pi{\sigma_y}^2} \tag{8}$$

Consideration of the most unfavourable case of hardness and fracture toughness values, and assuming a yield strength value of $H/3$, size of the

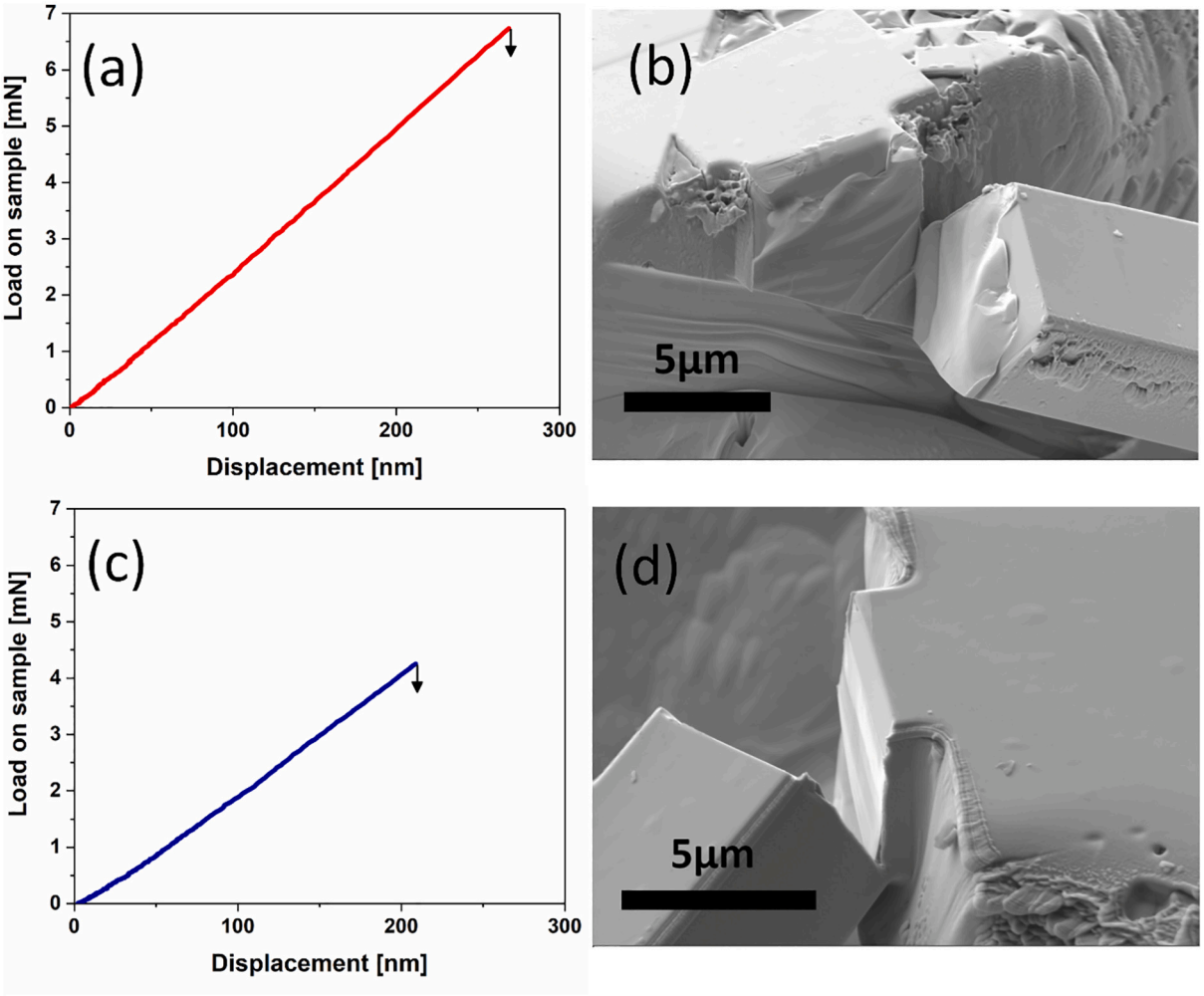

Fig. 4. Load-displacement curve corresponding to microcantilever bending test), and SEM image of broken specimen. of prismatic (a) and (b) and basal (c) and (d) orientations.

Table 2
Crystallographic orientation, dimensions, critical load and fracture toughness value calculated using experimental data attained for each microcantilever bending test conducted.

Orientation	D [µm]	b [µm]	W [µm]	a [µm]	P [mN]	K_{Ic} [MPa·m$^{1/2}$]
Prismatic	15.1	4.0	5.8	1.5	3.4	5.5
Prismatic	15.5	3.9	5.9	1.1	4.3	5.9
Prismatic	15.5	3.9	5.9	0.8	4.6	5.5
Basal	16.2	3.9	5.8	1.0	3.8	5.0
Basal	15.5	4.7	6.1	1.0	6.7	6.4

Table 3
Crystallographic orientation, dimensions, γ coefficient, critical load, and fracture toughness value calculated using experimental data attained for each pillar splitting test conducted.

Orientation	R [µm]	Height [µm]	γ coefficient	P_c [mN]	K_{Ic} [MPa·m$^{1/2}$]
Prismatic	2.2	4.5	0.46	33.9	4.9
Prismatic	2.2	4.3	0.46	42.1	6.0
Prismatic	2.7	6.0	0.46	53.2	5.7
Prismatic	2.7	6.4	0.46	37.7	3.9
Basal	2.8	5.8	0.40	36.7	3.3
Basal	2.5	6.1	0.40	14.7	1.5
Basal	2.6	5.5	0.40	29.3	2.9

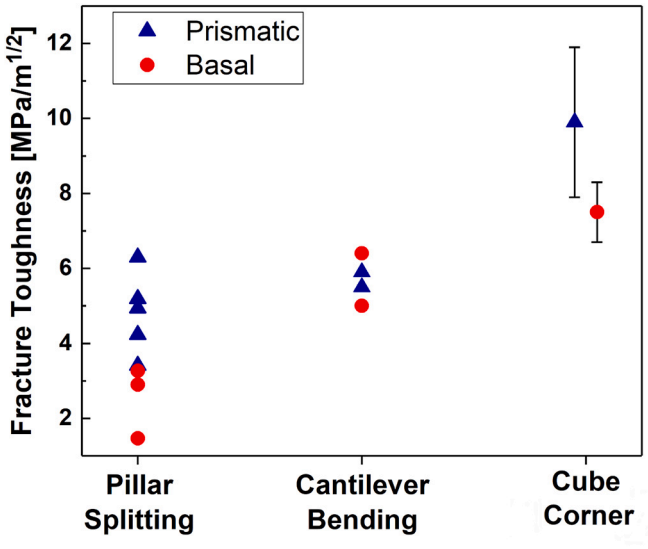

Fig. 5. Fracture toughness values of single WC grains obtained with different techniques. Fracture toughness vàlues estimated by cube corner indentation are obtained from [21].

Table 4
Average values of fracture toughness measured. Different crystallographic orientations are distinguished for the results attained using the micropillar splitting method.

Testing method	Average K_{Ic} [MPa·m$^{1/2}$]
Microcantilever bending	5.6 ± 0.8
Micropillar splitting (prismatic)	5.1 ± 1.0
Micropillar splitting (basal)	2.5 ± 1.0

plastic zone is estimated to be around 0.16 μm. Such a value is smaller than both notch length and dimensions of the milled microcantilevers. More accurate predictions of the plastic zone based on the model of Jia et al. [37] gives similar results on the order of 0.15 μm. Therefore, values obtained from microcantilever bending tests can be considered to fulfil the requirements of linear elastic fracture mechanics. They are lower than the ones obtained by means of the IM method, and relative differences could be explained by considering the plastic deformation features evidenced within and around indentation imprints, as well as the irregular cracking patterns observed in single WC grains.

The mean value determined for the K_{Ic} of WC using the microcantilever bending method −5.6 ± 0.8 MPa·m$^{1/2}$ - can be considered as relatively high for ceramic materials, although in the range of those usually found in tough advanced structural ceramics, such as zirconia [38]. However, considering the dislocation slip and plastic deformation capability shown by this material, as referred to above and previously reported in the literature (e.g. Refs. [39]) it should be somehow expected. Regarding reliability of the measured value, it should be highlighted that it is in satisfactory agreement with values reported in the literature which have been indirectly estimated from other macromechanical tests. Warren aimed to evaluate the fracture properties of several brittle solids, including WC single crystals, by Hertzian indentation [40]. In doing so, and after implementing some numerical modelling for analysing his experimental findings, values between 3 and 6 MPa·m$^{1/2}$ for WC, depending on the fitting parameters, were reported. This value is close to the ones reported by other indirect methods. More recently, Tarrago et al. [41] found a best-fit value of 7.5 MPam$^{1/2}$ for the K_{Ic} of WC grains, when developing an analytical representation of the evolution of bridging stress as a function of experimentally measured crack opening displacement, through FIB/FESEM serial sectioning and imaging of crack–microstructure interaction in cracks arrested after stable extension under monotonic loading. The slightly higher value reported can be attributed to experimental scatter of the small-scale measurements, the particular model used or to the fact that in this case K_{Ic} definition (for triggering initial crack extension within R-curve behaviour) included WC/binder issues. Furthermore, a lower-limit value of 5.8 MPam$^{1/2}$ has been estimated for the fatigue crack growth threshold (K_{th}) of a widely range of microstructurally different cemented carbides [42]. Considering that, different from other extrinsically-toughened brittle materials, strength lessening under cyclic loads of cemented carbides can be rationalized by suppression of toughening mechanisms, mainly derived from plastic stretching of crack-bridging ductile enclaves developed under monotonic loading, rather than degradation of them [43] the referred (K_{th}) could then be directly linked to the K_{Ic} of the binderless-like contiguous WC skeleton. Finally, following the results presented in Refs. [26, 44] on the strength of unnotched microcantilevers - in the range between 4 and 25 GPa – a critical defect size in the order of magnitude of tenths of nanometers may be estimated. This is coherent with the fractographic findings reported in these works, where no evident defect can be appreciated by SEM inspection and with initial defects initiated by plastic accumulation, as argued in [28].

5. Conclusions

Bending of notched microcantilevers has shown to be a successful technique to assess the fracture toughness of single WC grains embedded within the phase assemblage of cemented carbides. Fractographic inspection of broken specimens permits to evidence a purely brittle fracture, and no apparent artefacts are produced during the test. The average value measured is 5.6 MPa·m$^{1/2}$ and, with the current set of experiments, crystal orientation effects on fracture toughness are not discerned. Reliability of measured values is supported by the satisfactory agreement of them with those estimated indirectly from alternative macromechanical tests, such as Hertzian indentation, growth resistance of indentation cracks, and fatigue crack growth behaviour of through-thickness cracks. More precision in the fracture toughness values measured, as well as determination of its possible dependence with crystal orientation, may be acquired by testing a larger number of samples or trying other small-scale testing techniques.

On the other hand, indentation methods do not seem suitable to measure the fracture toughness of WC particles. Local plasticity exhibited by these crystals, and its corresponding anisotropy nature, yield asymmetric cracking systems. It implies that assumptions for analysis of experimental findings from pillar splitting and IM testing are not completely fulfilled. As a consequence, fracture toughness values measured using these methods are not completely reliable for single WC grains.

Author statement

I hereby declare that all changes have been done in agreement with the rest of authors.

Declaration of Competing Interest

The authors declare that they have no known competing financial interests or personal relationships that could have appeared to influence the work reported in this paper.

Acknowledgments

Work funded in part by the Spanish Ministerio de Ciencia, Innovación y Universidades (Spain) through grant PGC2018-096855-B-C41.

References

[1] L. Prakash, Fundamentals and general applications of hardmetals, in: Compr. Hard Mater., Elsevier Ltd., 2014, pp. 29–90, https://doi.org/10.1016/B978-0-08-096527-7.00002-7.
[2] H.E. Exner, Physical and chemical nature of cemented carbides, Int. Met. Rev. 24 (1979) 149–170, https://doi.org/10.1179/imtr.1979.24.1.149.
[3] A.J. Gant, R. Morrell, A.S. Wronski, H.G. Jones, Edge toughness of tungsten carbide based hardmetals, Int. J. Refract. Met. Hard Mater. 75 (2018) 262–278, https://doi.org/10.1016/j.ijrmhm.2017.12.020.
[4] M.G. Gee, A. Gant, B. Roebuck, Wear mechanisms in abrasion and erosion of WC/co and related hardmetals, Wear. 263 (2007) 137–148, https://doi.org/10.1016/j.wear.2006.12.046.
[5] J.M. Tarragó, E. Jimenez-Piqué, M. Turón-Vinas, L. Rivero, I. Al-dawery, L. Schneider, L. Llanes, Fracture and fatigue behaviour of cemented carbides: 3D focused ion beam tomography of crack-microstructure interactions, Int. J. Powder Metall. 50 (2014) 1–10.
[6] K. Yalamanchili, F. Wang, H. Aboulfadl, J. Barrirero, L. Rogstrom, E. Jimenez-Pique, F. Mücklich, F. Tasnadi, M. Odén, N. Ghafoor, Growth and thermal stability of TiN/ZrAlN: effect of internal interfaces, Acta Mater. 121 (2016) 396–406, https://doi.org/10.1016/j.actamat.2016.07.006.
[7] J.M. Tarragó, D. Coureaux, Y. Torres, E. Jiménez-Piqué, L. Schneider, J. Fair, L. Llanes, Strength and reliability of WC-Co cemented carbides: understanding microstructural effects on the basis of R-curve behavior and fractography, Int. J. Refract. Met. Hard Mater. 71 (2018) 221–226, https://doi.org/10.1016/j.ijrmhm.2017.11.031.
[8] H. Zhang, Z.Z. Fang, J.D. Belnap, Quasi-plastic deformation of WC-co composites loaded with a spherical indenter, Metall. Mater. Trans. A Phys. Metall. Mater. Sci. 38 (2007) 552–561, https://doi.org/10.1007/s11661-006-9036-y.
[9] B. Roebuck, E.A. Almond, Deformation and fracture processes and the physical metallurgy of WC-co hardmetals, Int. Mater. Rev. 33 (1988) 90–112, https://doi.org/10.1179/imr.1988.33.1.90.

[10] J.M. Tarragó, J.J. Roa, V. Valle, J.M. Marshall, L. Llanes, Fracture and fatigue behavior of WC-Co and WC-CoNi cemented carbides, Int. J. Refract. Met. Hard Mater. 49 (2015) 184–191, https://doi.org/10.1016/j.ijrmhm.2014.07.027.
[11] L. Llanes, Y. Torres, M. Anglada, On the fatigue crack growth behavior of WC-Co cemented carbides: Kinetics description, microstructural effects and fatigue sensitivity, Acta Mater. (2002) 2381–2393, https://doi.org/10.1016/S1359-6454(02)00071-X.
[12] L.S. Sigl, H.F. Fischmeister, On the fracture toughness of cemented carbides, Acta Metall. 36 (1988) 887–897, https://doi.org/10.1016/0001-6160(88)90143-5.
[13] J. Jang, G.M.M. Pharr, Influence of indenter angle on cracking in Si and Ge during nanoindentation, Acta Mater. 56 (2008) 4458–4469, https://doi.org/10.1016/j.actamat.2008.05.005.
[14] G.M. Pharr, Measurement of mechanical properties by ultra-low load indentation, Mater. Sci. Eng. A 253 (1998) 151–159, https://doi.org/10.1016/S0921-5093(98)00724-2.
[15] D.B. Marshall, R.F. Cook, N.P. Padture, M.L. Oyen, A. Pajares, J.E. Bradby, I. E. Reimanis, R. Tandon, T.F. Page, G.M. Pharr, B.R. Lawn, The compelling case for indentation as a functional exploratory and characterization tool, J. Am. Ceram. Soc. 98 (2015) 2671–2680, https://doi.org/10.1111/jace.13729.
[16] N. Cuadrado, D. Casellas, M. Anglada, E. Jiménez-Piqué, Evaluation of fracture toughness of small volumes by means of cube-corner nanoindentation, Scr. Mater. 66 (2012) 670–673, https://doi.org/10.1016/j.scriptamat.2012.01.033.
[17] D. Casellas, J. Caro, S. Molas, J.M. Prado, I. Valls, Fracture toughness of carbides in tool steels evaluated by nanoindentation, Acta Mater. 55 (2007) 4277–4286, https://doi.org/10.1016/j.actamat.2007.03.028.
[18] D.K. Shetty, I.G. Wright, P.N. Mincer, A.H. Clauer, Indentation fracture of WC-co cermets, J. Mater. Sci. 20 (1985) 1873–1882, https://doi.org/10.1007/BF00555296.
[19] G.D. Quinn, R.C. Bradt, On the vickers indentation fracture toughness Test, J. Am. Ceram. Soc. (2007) 673–680, https://doi.org/10.1111/j.1551-2916.2006.01482.x.
[20] N. Cuadrado, J. Seuba, D. Casellas, M. Anglada, E. Jiménez-Piqué, Geometry of nanoindentation cube-corner cracks observed by FIB tomography: implication for fracture resistance estimation, J. Eur. Ceram. Soc. 35 (2015) 2949–2955, https://doi.org/10.1016/j.jeurceramsoc.2015.03.031.
[21] N. Cuadrado, D. Casellas, L. Llanes, I. Gonzalez, J. Caro, Effect of crystal anisotropy on the mechanical properties of WC embedded in WC-Co cemented carbides, in: Proc. Euro PM2011 Powder Metall. Congr. Exhib., 2011, pp. 215–220. https://www.researchgate.net/publication/277104095 (accessed November 4, 2020).
[22] D. Di Maio, S.G.G. Roberts, Measuring fracture toughness of coatings using focused-ion-beam-machined microbeams, J. Mater. Res. 20 (2011) 299–302, https://doi.org/10.1557/JMR.2005.0048.
[23] G. Žagar, V. Pejchal, M.G. Mueller, L. Michelet, A. Mortensen, Fracture toughness measurement in fused quartz using triangular chevron-notched micro-cantilevers, Scr. Mater. 112 (2016) 132–135, https://doi.org/10.1016/j.scriptamat.2015.09.032.
[24] A.D. Norton, S. Falco, N. Young, J. Severs, R.I. Todd, Microcantilever investigation of fracture toughness and subcritical crack growth on the scale of the microstructure in Al 2 O 3, J. Eur. Ceram. Soc. 35 (2015) 4521–4533, https://doi.org/10.1016/j.jeurceramsoc.2015.08.023.
[25] M.R. Elizalde, I. Ocaña, J. Alkorta, J.M. Sánchez-Moreno, Mechanical strength assessment of single WC-WC interfaces present in WC-co hardmetals through micro-beam bending experiments, Int. J. Refract. Met. Hard Mater. 72 (2018) 39–44, https://doi.org/10.1016/j.ijrmhm.2017.12.009.
[26] M. Trueba, A. Aramburu, N. Rodríguez, I. Iparraguirre, M.R. Elizalde, I. Ocaña, J. M. Sánchez, J.M. Martínez-Esnaola, "in-situ" mechanical characterisation of WC-Co hardmetals using microbeam testing, Int. J. Refract. Met. Hard Mater. 43 (2014) 236–240, https://doi.org/10.1016/j.ijrmhm.2013.12.005.
[27] J.J. Roa, R. Rodríguez, V. Lamelas, R. Martínez, E. Jiménez-Piqué, L. Llanes, Small scale fracture behaviour of multilayer TiN/CrN systems: assessment of bilayer thickness effects by means of ex-situ tests on FIB-milled micro-cantilevers, Surf. Coat. Technol. 308 (2016) 414–417, https://doi.org/10.1016/j.surfcoat.2016.06.093.
[28] J. Ast, M. Ghidelli, K. Durst, M. Göken, M. Sebastiani, A.M. Korsunsky, A review of experimental approaches to fracture toughness evaluation at the micro-scale, Mater. Des. 173 (2019) 1007766, https://doi.org/10.1016/j.matdes.2019.107762.
[29] M. Sebastiani, K.E. Johanns, E.G. Herbert, F. Carassiti, G.M. Pharr, A novel pillar indentation splitting test for measuring fracture toughness of thin ceramic coatings, Philos. Mag. 95 (2015) 1928–1944, https://doi.org/10.1080/14786435.2014.913110.
[30] M. Sebastiani, K.E. Johanns, E.G. Herbert, G.M. Pharr, Measurement of fracture toughness by nanoindentation methods: recent advances and future challenges, Curr. Opin. Solid State Mater. Sci. 19 (2015) 324–333, https://doi.org/10.1016/j.cossms.2015.04.003.
[31] A. Krawitz, E. Drake, Residual stresses in cemented carbides - an overview, Int. J. Refract. Met. Hard Mater. 49 (2015) 27–35, https://doi.org/10.1016/j.ijrmhm.2014.07.018.
[32] E. Jiménez-Piqué, M. Turon-Vinas, H. Chen, T. Trifonov, J. Fair, E. Tarrés, L. Llanes, Focused ion beam tomography of WC-co cemented carbides, Int. J. Refract. Met. Hard Mater. 67 (2017) 9–17, https://doi.org/10.1016/j.ijrmhm.2017.04.007.
[33] M. Ghidelli, M. Sebastiani, K.E. Johanns, G.M. Pharr, Effects of indenter angle on micro-scale fracture toughness measurement by pillar splitting, J. Am. Ceram. Soc. 100 (2017) 5731–5738, https://doi.org/10.1111/jace.15093.
[34] L. Llanes, In-Depth Understanding of Fatigue Micromechanisms in Cemented Carbides, Metals (Basel). 9 (2019) 924–933.
[35] J.J. Roa, E. Jimenez-Pique, C. Verge, J.M. Tarrago, A. Mateo, J. Fair, L. Llanes, Intrinsic hardness of constitutive phases in WC-co composites: Nanoindentation testing, statistical analysis, WC crystal orientation effects and flow stress for the constrained metallic binder, J. Eur. Ceram. Soc. 35 (2015) 3419–3425, https://doi.org/10.1016/j.jeurceramsoc.2015.04.021.
[36] T. Csanádi, M. Bľanda, A. Duszová, N.Q. Chinh, P. Szommer, J. Dusza, Deformation characteristics of WC micropillars, J. Eur. Ceram. Soc. 34 (2014) 4099–4103, https://doi.org/10.1016/j.jeurceramsoc.2014.05.045.
[37] Y.J. Jia, M.X. Shi, Y. Zhao, B. Liu, A better estimation of plastic zone size at the crack tip beyond Irwin's model, J. Appl. Mech. Trans. ASME. 80 (2013), https://doi.org/10.1115/1.4023642.
[38] M. Turon-Vinas, M. Anglada, Strength and fracture toughness of zirconia dental ceramics, Dent. Mater. 34 (2018) 365–375, https://doi.org/10.1016/j.dental.2017.12.007.
[39] S. Bartolucci-Luyckx, Microscopic aspects of fracture in WC-Co alloys, Acta Metall. 16 (1968) 535–544.
[40] R. Warren, Measurement of the fracture properties of brittle solids by hertzian indentation, Acta Metall. 26 (1978) 1759–1769, https://doi.org/10.1016/0001-6160(78)90087-1.
[41] J.M. Tarragó, E. Jiménez-Piqué, L. Schneider, D. Casellas, Y. Torres, L. Llanes, FIB/FESEM experimental and analytical assessment of R-curve behavior of WC–co cemented carbides, Mater. Sci. Eng. A 645 (2015) 142–149, https://doi.org/10.1016/j.msea.2015.07.090.
[42] J.M. Tarragó, J.J. Roa, V. Valle, J.M. Marshall, L. Llanes, Fracture and fatigue behavior of WC-Co and WC-CoNi cemented carbides, Int. J. Refract. Met. Hard Mater. 49 (2015) 184–191, https://doi.org/10.1016/j.ijrmhm.2014.07.027.
[43] J.M. Tarragó, E. Jiménez-Piqué, M. Turón, L. Rivero, L. Llanes, I. Al-Dawery, L. Schneider, Fracture and fatigue behavior of cemented carbides: 3-D FIB tomography of crack-microstructure interactions, in: Adv. Tungsten, Refract. Hardmaterials IX - Proc. 9th Int. Conf. Tungsten, Refract. Hardmaterials, 2014.
[44] T. Csanádi, M. Vojtko, J. Dusza, Deformation and fracture of WC grains and grain boundaries in a WC-Co hardmetal during microcantilever bending tests, in: Int. J. Refract. Met. Hard Mater. 87, 2020, https://doi.org/10.1016/j.ijrmhm.2019.105163.